

SPEED VARIATIONS IN CAGE INDUCTION MOTORS UNDER SINUSOIDAL VOLTAGE MODULATION

Piotr Gnaciński¹, Damian Hallmann^{2*}

Gdynia Maritime University, 83 Morska St., 81–225 Gdynia, Poland,
Faculty of Electrical Engineering, Department of Marine Electrical Power Engineering

¹ email: p.gnacinski@we.umg.edu.pl, ORCID 0000-0003-3903-0453

² email: d.hallmann@we.umg.edu.pl, ORCID 0000-0003-4129-8336

* Corresponding author

Abstract: A specific case of voltage fluctuations is sinusoidal voltage modulation, which is a superposition of the fundamental voltage component and the subharmonic and interharmonic components – that is components of frequency less than the fundamental one or not being an integer multiple of it. Depending on the phase angles of the subharmonic and interharmonic components, various cases of voltage modulation can be distinguished, like amplitude, phase and intermediate modulations. This paper deals with the effect of phase angles of the subharmonic and interharmonic components on speed variation. The results of FEM computations are presented for a cage induction motor with a rated power of 3 kW.

Keywords: cage induction motor, finite element method, interharmonics, power quality, rotational speed, subharmonics, voltage fluctuations.

1. INTRODUCTION

Voltage fluctuations are considered one of the most important and most frequent power quality disturbances [Bollen and Gu 2006; Ghaseminezhad et al. 2021a,b; Kuwałek 2021; Patel and Chowdhury 2021]. Usually they are defined as quick changes in the effective voltage value [Bollen and Gu 2006; Ghaseminezhad et al. 2021a,b; Kuwałek 2021; Patel and Chowdhury 2021]. For regular voltage fluctuations, this definition corresponds to voltage amplitude modulation. The occurrence of voltage fluctuations is related to the operation of receivers drawing variable power over time, and to renewable sources of electric energy [Bollen and Gu 2006; Kovaltchouk et al. 2016].

A special case of voltage fluctuations is sinusoidal modulation. In practice, it is equivalent to the occurrence of additional components within the waveform [Gallo et al. 2005; Bollen and Gu 2006; Tennakoon, Perera and Robinson 2008; Ghaseminezhad et al. 2021a,b] – subharmonics and interharmonics – components

with a frequency lower than the fundamental component, and a component with a frequency that is not an integer multiple of the frequency of the fundamental component. Depending on the phase angles of the subharmonics and interharmonics, voltage fluctuations may take the form of modulation of amplitude, phase or an intermediate form [Gallo et al. 2005; Bollen and Gu 2006]. In cases where the function modulating the voltage does not have a sinusoidal waveform, it can be considered a superposition of sinusoids with different frequencies [Ghaseminezhad et al. 2021a,b].

Voltage subharmonics and interharmonics interfere with the operation of various elements of the power system – electronic equipment, light sources, power and measurement transformers, automation systems, synchronous and asynchronous machines [Gallo et al. 2005; Testa et al. 2007; Tennakoon, Perera and Robinson 2008; Ghaseminezhad et al. 2017a,b; Gnaciński et al. 2019a,c; Gnaciński and Klimczak 2020; Hallmann 2020; Crotti et al. 2021; Ghaseminezhad et al. 2021a,b; Gnaciński et al. 2021a; Gnaciński, Muc and Pepliński 2021; Zhang 2021]. In asynchronous motors, they cause fluctuations in rotational speed and torque, increased power losses and winding temperatures, local saturation of the magnetic circuit and vibrations [Tennakoon, Perera and Robinson 2008; Ghaseminezhad et al. 2017a,b; Gnaciński et al. 2019a,b,c; Gnaciński and Klimczak 2020; Hallmann 2020; Ghaseminezhad et al. 2021a,b; Gnaciński et al. 2021a; Gnaciński, Muc and Pepliński 2021; Zhang 2021].

Currently, voltage quality standards do not specify an acceptable level of subharmonics or interharmonics. The standard *IEEE Recommended practice and requirements for harmonic control in electric power systems* [IEEE Standard 519 2014] only provides for information purposes the values of subharmonics and interharmonics corresponding to the maximum acceptable levels of light flickers and mentions that proper attention should be paid to the adverse effects of these interferences on generators, motors, transformers, etc. On the other hand, the standard PN-EN 50160 [EN 50160 2010] *Power voltage parameters in public power grids* includes the following comment: "levels are under consideration, pending more experience". To summarise, determining an acceptable level of the subharmonics and interharmonics requires in-depth research into the effects of these interferences on different elements of the power system.

Previous studies on asynchronous motors powered by a voltage containing subharmonics and interharmonics generally concerned either the effects of a single voltage subharmonic or interharmonic on an asynchronous motor [Tennakoon, Perera and Robinson 2008; Gnaciński et al. 2019a,b,c; Gnaciński and Klimczak 2020; Gnaciński et al. 2021a] or the effects of voltage amplitude modulation [Tennakoon, Perera and Robinson 2008; Ghaseminezhad et al. 2017a,b; 2021a,b], ignoring the phase angles of subharmonics and interharmonics. The following paper presents the effects of these phase angles on rotational speed fluctuations.

2. STUDY METHODOLOGY

Numerical calculations using the finite element method were adopted as the study methodology. A two-dimensional model of a TSg100L-4B motor (rated parameters of the motor are shown in Table 1) was implemented in the ANSYS Electronics Desktop environment.

The parameters of the model were identified based on the structural data and experimental results [Hallmann 2020]. In the calculations, a transient solver and a tau mesh were used.

The mesh used (Fig. 1) had 22094 triangular elements, and its density was selected based on solution convergence analysis [Hallmann 2020].

Experimental verification of the numerical model is presented in [Gnaciński et al. 2019a,b; Hallmann 2020; Gnaciński et al. 2021a], and its detailed description – in [Hallmann 2020] and [Gnaciński et al. 2019b; Hallmann 2020; Gnaciński et al. 2021a].

Table 1. Rated parameters of the TSg100L-4B test motor

Parameter	Value
Rated power	3 kW
Rated frequency	50 Hz
Rated voltage	380 V
Rated current	6.9 A
Rated power index	0.81
Rated speed	1420 rpm
Winding connection	delta

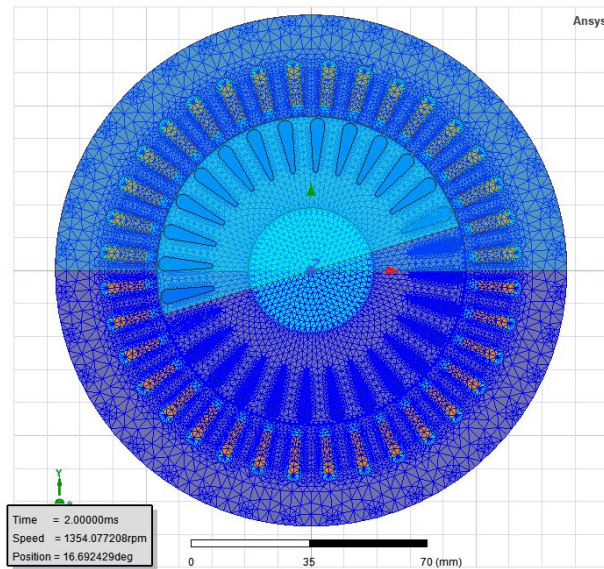


Fig. 1. Mesh used

Source: original study.

3. SINUSOIDAL VOLTAGE MODULATION AND ROTATIONAL SPEED FLUCTUATIONS

As has been mentioned in the Introduction, sinusoidal voltage modulation can also be treated as a superposition of the fundamental voltage component and the subharmonic and interharmonic components (based on [Gallo et al. 2005; Bollen and Gu 2006; Ghaseminezhad et al. 2021a,b]):

$$v(t) = V_1[\cos(2\pi f_1 t) + a \cos(2\pi f_{sh} t + \phi_{sh}) + a \cos(2\pi f_{ih} t + \phi_{ih})] \quad (1)$$

where:

V_1 – fundamental component amplitude;

a – ratio of voltage subharmonic and interharmonic amplitude to fundamental component amplitude;

ϕ_{sh} – phase angle of the subharmonic component;

ϕ_{ih} – phase angle of the interharmonic component;

f_1 – fundamental component frequency; f_{sh}, f_{ih} – frequency of the subharmonic and interharmonic, equal to:

$$f_{sh} = f_1 - f_m \quad (2)$$

$$f_{ih} = f_1 + f_m \quad (3)$$

where f_m – voltage modulation frequency.

It must be noted that for the waveform described by equation (1), amplitude modulation occurs for phase angles $\phi_{sh} + \phi_{ih} = 0$, while phase modulation occurs for $\phi_{sh} + \phi_{ih} = 180^\circ$ [Gallo et al. 2005].

Below are presented the test results on the effects of phase angles of subharmonics and interharmonics on rotational speed fluctuations. All numerical experiments were conducted for a relative subharmonic and interharmonic amplitude $a = 0.01$, angle $\phi_{sh} = 0$, anti-torque and fundamental voltage component with rated values ($T_n = 20.25$ Nm and $U_n = 380$ V), and load with a negligible moment of inertia (motor moment of inertia $J_s = 0.00702299$ kg m²; load moment of inertia $J_o = 0$ kg m²). Example test voltage waveforms are shown in Figure 2 and Figure 3.

Figure 4 shows the characteristic of rotational speed fluctuation amplitude as a function of angle ϕ_{ih} for voltage modulation frequency $f_m = 30$ Hz. It must be noted that for a given modulation frequency f_m the torque pulsation frequency corresponds to the natural frequency of the rigid-body mode (rotating masses) [Arkio et al. 2018]. For the resonance frequency, rotational speed fluctuations caused by voltage subharmonics and interharmonics amplify the current subharmonics and interharmonics, causing even greater fluctuations of torque and rotational speed, and consequently – a flow of current subharmonics and interharmonics with extremely high values, significant torque fluctuations and excessive vibrations [Hallmann 2020; Gnaciński et al. 2019a,c; Gnaciński and Klimczak 2020; Gnaciński et al. 2021a; Ghaseminezhad et al. 2021a,b].

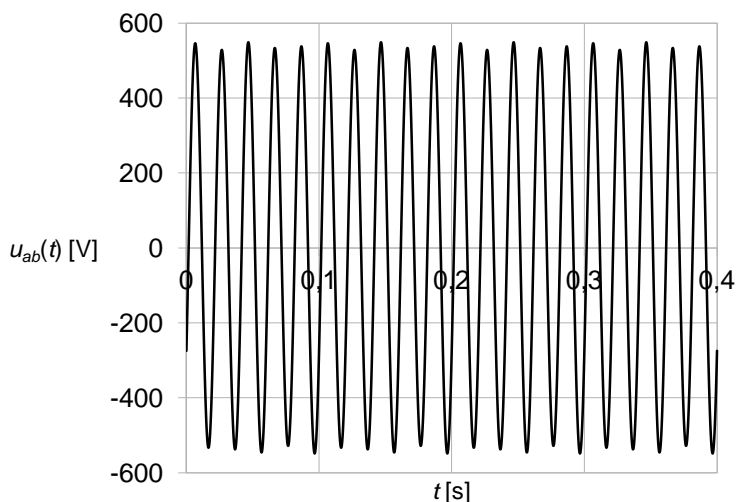


Fig. 2. Example test voltage waveform for angles $\phi_{sh} = 0$, $\phi_{ih} = 0$, and voltage modulation frequency $f_m = 20$ Hz

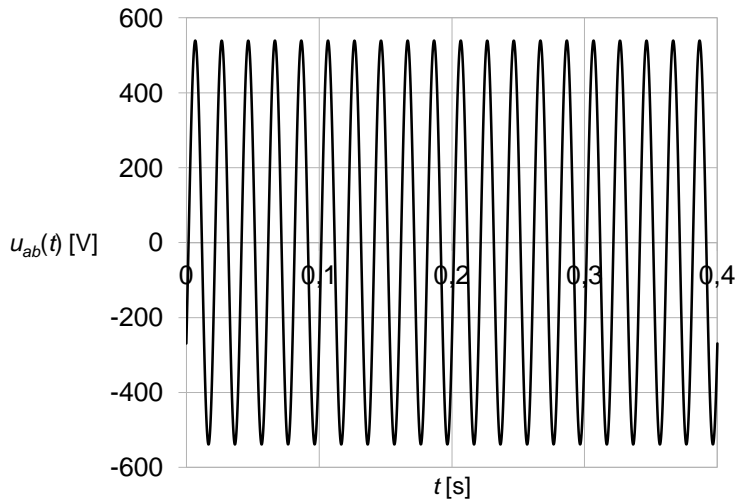


Fig. 3. Example test voltage waveform for angles $\phi_{sh} = 0$, $\phi_{ih} = 180^\circ$, and voltage modulation frequency $f_m = 20$ Hz

As demonstrated by the test results shown in Figure 4, rotational speed fluctuations significantly depend on the phase angles under consideration. The highest and lowest speed fluctuations (7.84% and 4.36%, respectively) occur for angles $\phi_{ih} = 270^\circ$ and $\phi_{ih} = 90^\circ$. The momentary speed value charts for these angles are shown in Figure 5 and Figure 6. The differences are consequences of the fact that for some phase angles, rotational speed fluctuations caused independently by the voltage subharmonic and interharmonic mutually amplify each other, while for others they attenuate each other.

The next figures (Fig. 7 and Fig. 8) show the characteristics of rotational speed fluctuation amplitude as a function of voltage modulation frequency f_m . The results in Fig. 7 apply to angle $\phi_{ih} = 0$ (amplitude modulation), and in Fig. 8 to angle $\phi_{ih} = 180^\circ$ (phase modulation). Furthermore, for the purpose of comparison, Fig. 9 presents the characteristics of rotational speed fluctuations as a function of voltage subharmonic frequency f_{sh} , which occurs as a power quality disturbance. For the test motor and phase modulation (Fig. 8), rotational speed fluctuations were generally slightly higher than that for amplitude modulation (Fig. 7), which in turn were slightly higher than for a single subharmonic. The above results may not be generalised to cover other motors. It must also be noted that rotational speed fluctuation peaks for frequency $f_m = 30$ Hz (Fig. 7 and Fig. 8) and $f_{sh} = 20$ Hz (Fig. 9) are caused by the above resonance phenomena.

To summarise, the phase angles of the subharmonics and interharmonics significantly affected rotational speed fluctuations.

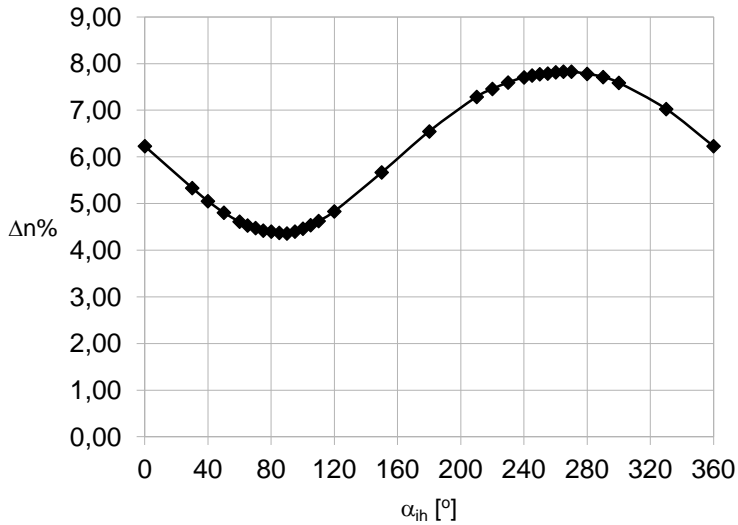


Fig. 4. Rotational speed fluctuation amplitude as a function of angle ϕ_{ih} for $\phi_{sh} = 0$ and voltage modulation frequency $f_m = 30$ Hz

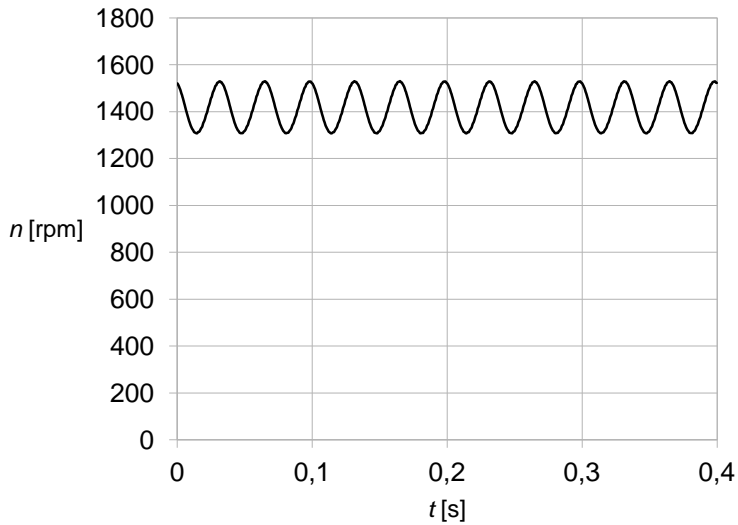


Fig. 5. Rotational speed for angles $\phi_{ih} = 270^\circ$, $\phi_{sh} = 0$ and voltage modulation frequency $f_m = 30$ Hz

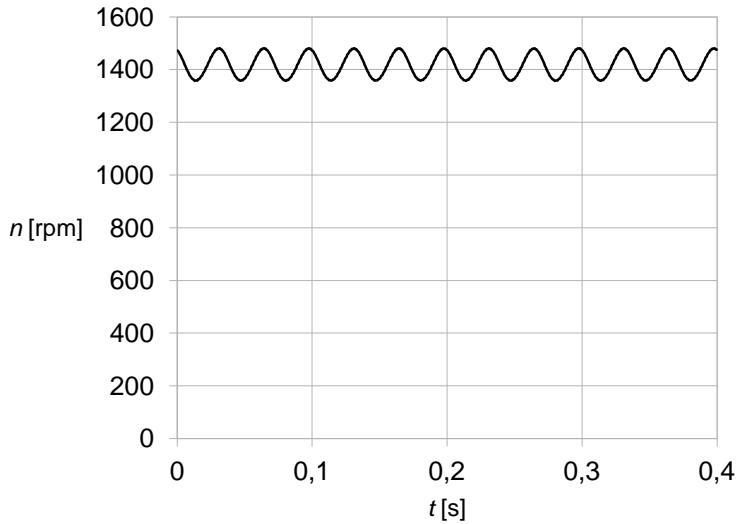


Fig. 6. Rotational speed for angles $\phi_{ih} = 90^\circ$, $\phi_{sh} = 0$ and voltage modulation frequency $f_m = 30$ Hz

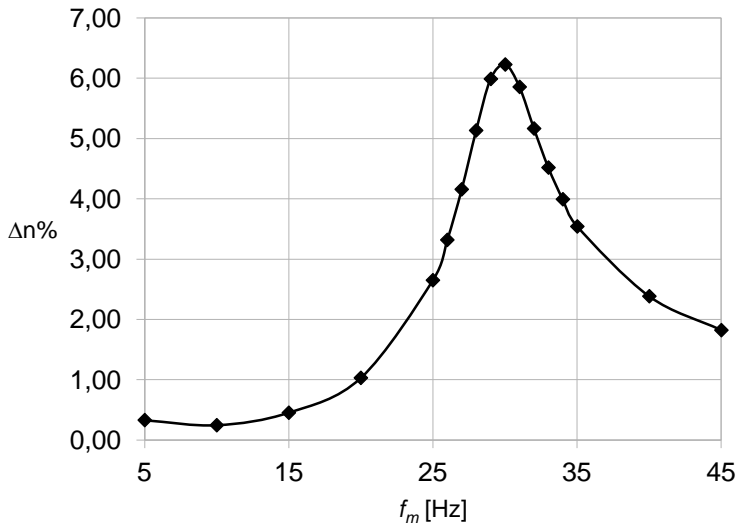


Fig. 7. Rotational speed fluctuation amplitude as a function of voltage modulation frequency f_m for angles $\phi_{sh} = 0$, $\phi_{ih} = 0$ (amplitude modulation)

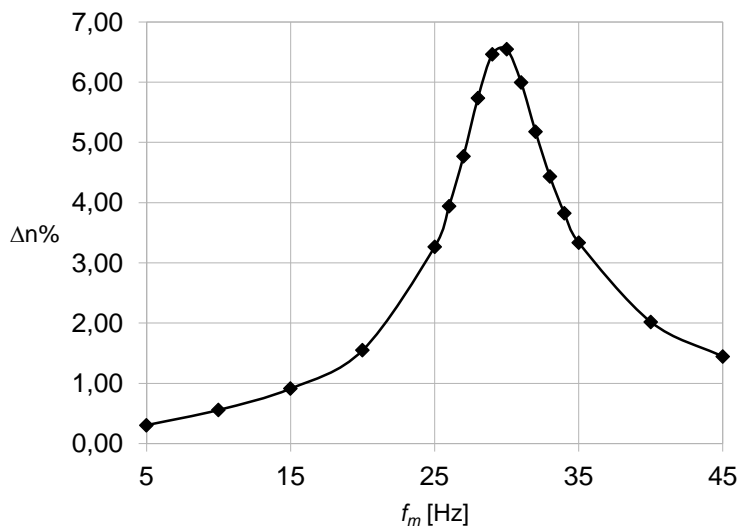


Fig. 8. Rotational speed fluctuation amplitude as a function of voltage modulation frequency f_m for angles $\phi_{sh} = 0$, $\phi_{th} = 180^\circ = 0$ (phase modulation)

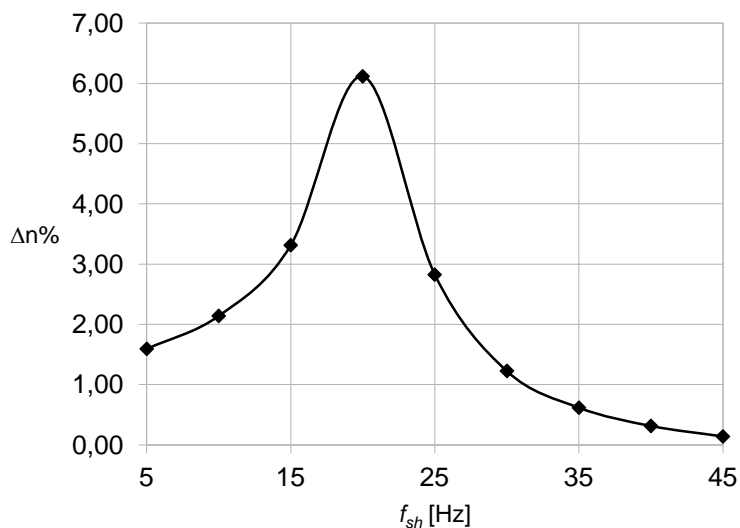


Fig. 9. Rotational speed fluctuation amplitude as a function of subharmonic frequency f_{sh} , occurring as a single power quality disturbance

4. CONCLUSIONS

The results demonstrate that rotational speed fluctuations under voltage modulation significantly depend on the phase angles of the voltage subharmonics and interharmonics. For some angles, speed fluctuations caused by the subharmonic and interharmonic mutually amplify each other, while for others they attenuate each other. For the test motor and the specific angles, the speed fluctuation amplitude was 80% higher than for others. The test results shown should contribute to a better understanding of the phenomena occurring in asynchronous motors affected by voltage fluctuations, in particular under fluctuation frequencies matching the natural frequency of the rigid-body mode (rotating masses).

REFERENCES

- Arkkio, A., Cederström, S., Awan, H.A.A., Saarakkala, S.E., Holopainen, T.P., 2018, *Additional Losses of Electrical Machines Under Torsional Vibration*, IEEE Transactions on Energy Conversion, Vol. 33, No. 1, pp. 245–251.
- Bollen, M.H.J., Gu, I.Y.H., 2006, *Signal Processing of Power Quality Disturbances*, Wiley, New York, USA.
- Crotti, G., D’Avanzo, G., Letizia, P.S., Luiso, M., 2021, *Measuring Harmonics with Inductive Voltage Transformers in the Presence of Subharmonics*, IEEE Transactions on Instrumentation and Measurement, Vol. 70, pp. 1–13.
- EN Standard 50160, 2010, *Voltage Characteristics of Electricity Supplied by Public Distribution Network*.
- Gallo, D., Landi, C., Langella, R., Testa, A., 2005, *Limits for Low Frequency Interharmonic Voltages: Can They Be Based on the Flickermeter Use*, IEEE Russia Power Tech, pp. 1–7.
- Ghaseminezhad, M., Doroudi, A., Hosseinian, S.H., Jalilian, A., 2017a, *Analysis of Voltage Fluctuation Impact on Induction Motors by an Innovative Equivalent Circuit Considering the Speed Changes*, IET Gener. Transm. Distrib., Vol. 11, pp. 512–519.
- Ghaseminezhad, M., Doroudi, A., Hosseinian, S.H., Jalilian, A., 2017b, *An Investigation of Induction Motor Saturation Under Voltage Fluctuation Conditions*, Journal of Magnetics, Vol. 22, pp. 306–314.
- Ghaseminezhad, M., Doroudi, A., Hosseinian, S.H., Jalilian, A., 2021a, *Analytical Field Study on Induction Motors Under Fluctuated Voltages*, Iranian Journal of Electrical and Electronic Engineering, Vol. 17, No. 1, pp. 1620–1620.
- Ghaseminezhad, M., Doroudi, A., Hosseinian, S.H., Jalilian, A., 2021b, *High Torque and Excessive Vibration on the Induction Motors Under Special Voltage Fluctuation Conditions*, COMPEL – The International Journal for Computation and Mathematics in Electrical and Electronic Engineering, Vol. 40, No. 4, pp. 822–836.
- Gnaciński, P., Hallmann, D., Klimczak, P., Muc, A., Pepliński, M., 2021, *Effects of Voltage Interharmonics on Cage Induction Motors*, Energies, Vol. 14, No. 5, pp. 12–18.
- Gnaciński, P., Hallmann, D., Pepliński, M., Jankowski, P., 2019a, *The Effects of Voltage Subharmonics on Cage Induction Machine*, International Journal of Electrical Power & Energy Systems, Vol. 111, pp. 125–131.

- Gnaciński, P., Klimczak, P., 2020, *High-Power Induction Motors Supplied with Voltage Containing Subharmonics*, *Energies*, Vol. 13, pp. 58–94.
- Gnaciński, P., Muc, A., Pepliński, M., 2021b, *Influence of Voltage Subharmonics on Line Start Permanent Magnet Synchronous Motor*, *IEEE Access*, Vol. 9, pp. 164 275–164 281.
- Gnaciński, P., Pepliński, M., Hallmann, D., Jankowski, P., 2019b, *Induction Cage Machine Thermal Transients Under Lowered Voltage Quality*, *IET Electric Power Applications*, Vol. 13, No. 4, pp. 479–486.
- Gnaciński, P., Pepliński, M., Murawski, L., Szeleziński, A., 2019c, *Vibration of Induction Machine Supplied with Voltage Containing Subharmonics and Interharmonics*, *IEEE Trans. Energy Convers.*, Vol. 34, pp. 1928–1937.
- Hallmann, D., 2020, *Analysis of Operation of an Induction Motor Supplied with Voltage Containing Subharmonics and Interharmonics Using a Field Model (in Polish)*, rozprawa doktorska, Uniwersytet Morski w Gdyni, Gdynia 2020.
- IEEE Standard 519-2014 (Revision of IEEE Standard 519-1992), 2014, *IEEE Recommended Practice and Requirements for Harmonic Control in Electric Power Systems*, IEEE, New York, USA.
- Kovaltchouk, T., Armstrong, S., Blavette, A., Ahmed, H.B., Multon, B., 2016, *Wave Farm Flicker Severity: Comparative Analysis and Solutions*, *Renewable Energy*, Vol. 91, pp. 32–39.
- Kuwałek, P., 2021, *Selective Identification and Localization of Voltage Fluctuation Sources in Power Grids*, *Energies*, Vol. 14, No. 20, pp. 65–85.
- Patel, D., Chowdhury, A., 2021, *Mitigation of Voltage Fluctuation in Distribution System using Sen Transformer with Variable Loading Conditions*, *International Conference on Advances in Electrical, Computing, Communication and Sustainable Technologies (ICAECT)*, pp. 1–6.
- Tennakoon, S., Perera, S., Robinson, D., 2008, *Flicker Attenuation – Part I: Response of Three-Phase Induction Motors to Regular Voltage Fluctuations*, *IEEE Transactions Power Delivery*, Vol. 23, pp. 1207–1214.
- Testa, A., et al. (21 authors), 2007, *Interharmonics: Theory and Modeling*, *IEEE Transactions Power Delivery*, Vol. 22, pp. 2335–2348.
- Zhang, S., Kang, J., Yuan, J., 2021, *Analysis and Suppression of Oscillation in V/F Controlled Induction Motor Drive Systems*, *IEEE Transactions on Transportation Electrification*, Vol. 8, pp. 1566–1574.



HIGH-SPEED BINARY-TO-RESIDUE CONVERTER DESIGN USING 2-BIT SEGMENTATION OF THE INPUT WORD

Robert Smyk^{1*}, Maciej Czyżak²

¹ Gdańsk University of Technology, 11/12 Gabriela Narutowicza Street, 80-233 Gdańsk, Poland, e-mail: robert.smyk@pg.edu.pl, ORCID 0000-0001-9365-4633

² The University of Applied Sciences in Elbląg, 1 Wojska Polskiego Street, 82-300 Elbląg, Poland, ORCID 0000-0002-2249-1619

*Corresponding author

Abstract: In this paper a new approach to the design of the high-speed binary-to-residue converter is proposed that allows the attaining of high pipelining rates by eliminating memories used in modulo m generators. The converter algorithm uses segmentation of the input binary word into 2-bit segments. The use and effects of the input word segmentation for the synthesis of converters for five-bit moduli are presented. For the number represented by each segment, the modulo m reduction using a segment modulo m generator is performed. The use of 2-bit segments substantially reduces the hardware amount of the layer of input modulo m generators. The generated residues are added using the multi-operand modulo m adder based on the carry-save adder (CSA) tree, reduction of the number represented by the output CSA tree vectors to the $2m$ range and fast two-operand modulo m additions. Hardware amount and time delay analyses are also included.

Keywords: Binary-to-residue conversion, residue number system, FPGA.

1. INTRODUCTION

The Residue Number System (*RNS*) [Szabo and Tanaka 1967; Cardarilli, Nannarelli and Re 2007; Luan 2014] is a non-weighted number system that allows the fast realization of addition, subtraction and multiplication without carries between the digits of the number. The *RNS* had its beginnings in ancient China, but renewed interest at the end of the 1950s arose when its application for multiplication and fault detection in computers was examined [Szabo and Tanaka 1967]. There were also attempts to design *RNS* arithmetic units for general-purpose computers, but difficulties in the realization of operations like division, sign determination, magnitude comparison and conversion to weighted systems limited the use of the *RNS* to the selected areas of cryptography and digital signal processing, where it could be useful for high-speed signal processors. The other applications are in low-power [Cardarilli, Nannarelli and Re 2007] and fault-tolerant arithmetics [Luan 2014]. Usually, the input to residue processors is encoded in the weighted system,